Electronic Supplementary Material (ESI) for Physical Chemistry Chemical Physics.

Supplementary Information

The effect of regioisomerism on the photophysical properties of alkylated-naphthalene liquids

Bhawani Narayan,[a] Kazuhiko Nagura,[a] Tomohisa Takaya,[b] Koichi Iwata,[b] Akira Shinohara,[c] Hideyuki Shinmori,[c] Hao Wang,[d] Quan Li,[d] Xiaofeng Sun,[e] Hongguang Li,[e] Shinsuke Ishihara[a] and Takashi Nakanishi*[a]

[a] Frontier Molecules Group, International Centre for Materials Nanoarchitectonics (WPI-MANA), National Institute for Materials Science (NIMS), 1-1 Namiki, Tsukuba 305-0044, Japan.

[b] Department of Chemistry, Faculty of Science, Gakushuin University, 1-5-1 Mejiro, Toshima-ku, Tokyo 171-8588, Japan.

[c] Department of Biotechnology, Interdisciplinary Graduate School of Medicine and Engineering University of Yamanashi, 4-4-37 Takeda, Kofu 400-8510, Japan.

[d] Liquid Crystal Institute, Kent State University, 1425 University Esplanade, Kent, OH 44242-0001, USA.

[e] Lanzhou Institute of Chemical Physics, Chinese Academy of Sciences, No.18 Tianshui Middle Road, Lanzhou 730000, P.R. China.

*E-mail: NAKANISHI.Takashi@nims.go.jp

Table of Contents

1. Supplementary Methods

1.1 Materials

Unless otherwise stated, all starting materials and reagents were purchased from commercial suppliers and used without further purification. All reactions were performed under an argon atmosphere. Silica-gel column chromatography was performed using Kanto Chemical silica gel 60 N (spherical, neutral). Spectroscopic grade solvents, dichloromethane (DOJINDO) and *n*-hexane (DOJINDO) were used for all spectroscopic studies without further purification. Commercially available 1-hydroxy naphthalene and 2-hydroxy naphthalene were purchased from TCI were recrystallized using a mixture of chloroform and cyclohexane before use. For the recrystallization of 1-hydroxy naphthalene, a mixture of $CHCl_3$:cyclohexane (1:3) was used while for the recrystallization of 2-hydroxy naphthalene, a mixture of $CHCl_3$:cyclohexane (1:1) was used. White needle shaped crystals were obtained in the case of 1-hydroxy naphthalene off-white flaky crystals were obtained in the case of 2-hydroxy naphthalene.

1.2 Synthesis and Characterization

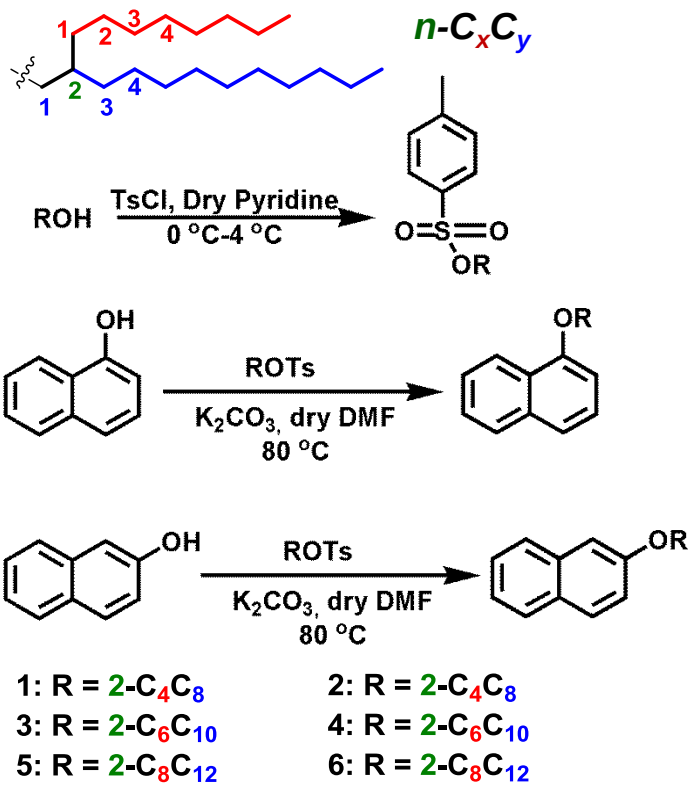

Scheme S1. General synthetic scheme for regioisomeric alkylated-naphthalene liquids (**1**–**6**).

1.2.1 General synthetic procedure for the tosylation of alcohols

The corresponding branched chain alcohol ROH was taken in a 100 mL two-necked flask. Air was replaced by argon gas from the flask by three times of vacuum-argon cycles. Then dry pyridine (0.4 mL / mmol) was added to the flask and the mixture was stirred for 10 minutes on an ice bath. To this, TsCl (0.95 equiv.) was added in parts under the flow of argon. The reaction mixture was stirred on ice bath for an average of 12 hours. The reaction was terminated based on TLC monitoring and ^{1}H NMR after a mini work up. 4 N HCl was added into the product mixture to neutralize the redundant pyridine. The resultant residue was extracted with hexane and washed several times with brine and water, dried over anhydrous Na_2SO_4. Evaporation of the organic layer under reduced pressure followed by column chromatography (hexane/chloroform = 70:30) over silica gel yielded pure tosylate.

This procedure for the C_4C_8 tosylate is reported elsewhere.[1] Similar protocol was followed for all the tosylates. The ^{1}H NMR results matched well with the reported ones.[2]

1.2.2 General synthetic procedure for the alkylation of naphthalenes

The recrystallized naphthol was taken in a 100 mL two-neck flask. Air was replaced by argon gas from the flask by three times of vacuum-argon cycles. Then, anhydrous dimethylformamide (DMF) was injected into the flask under argon flow. The reaction mixture was stirred at 80 °C for 12 hours. The reaction was monitored periodically with thin layer chromatography. The completion of the reaction was marked by the disappearance of the starting material and the formation of the product spot. The resultant residue was extracted with dichloromethane and washed several times with brine and water, dried over anhydrous Na_2SO_4. Evaporation of the organic layer under reduced pressure followed by column chromatography (hexane) over silica gel yielded the pure liquid naphthalene.

1: Colourless oil; ^{1}H NMR (400 MHz, $CDCl_3$): δ = 8.34 (d, 1H, J = 9.6 Hz); 7.84 (d, 1H, J = 8.4 Hz); 7.53-7.40 (m, 4H); 6.86 (d, 1H, J = 7.2 Hz); 4.06 (d, 2H, J = 5.6 Hz); 2.05-1.88 (m, 1H), 1.66-1.34 (m, 16H), 0.96-0.93 (m, 6H).

^{13}C NMR (100 MHz, $CDCl_3$): δ = 155.9, 134.6, 127.6, 126.4, 126.1, 125.9, 125.2, 122.3, 120.0, 104.5, 70.8, 38.2, 32.0, 31.8, 31.5, 29.9, 29.3, 27.1, 23.4, 23.3, 22.9, 14.3

MALDI-ToF MS (matrix: dithranol) calculated for $C_{22}H_{32}O$: 312.3, found: 312.4 $[M]^+$.

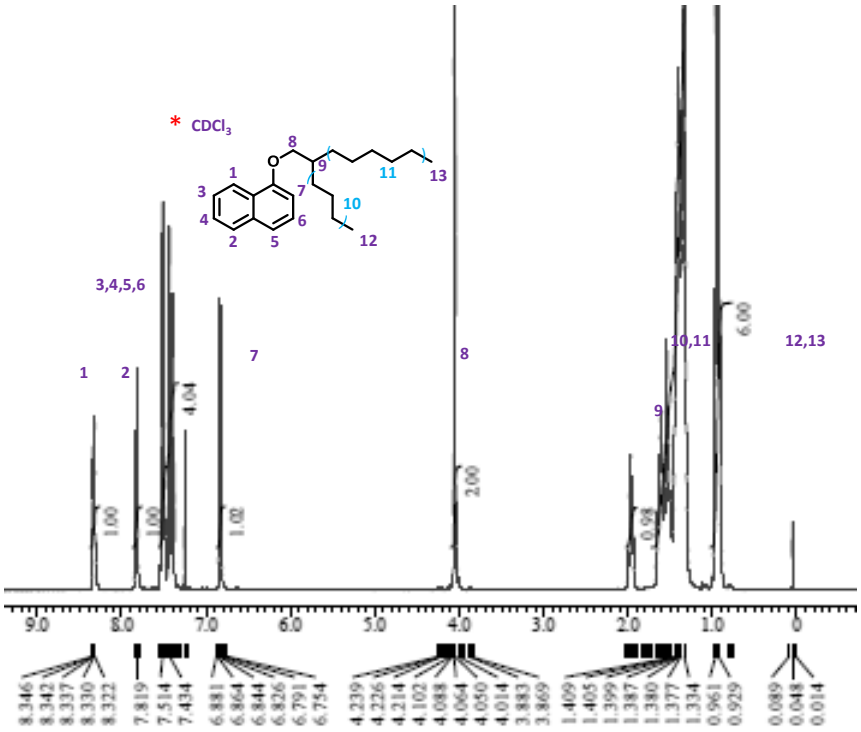

Fig. S1. ^{1}H NMR spectrum of **1**.

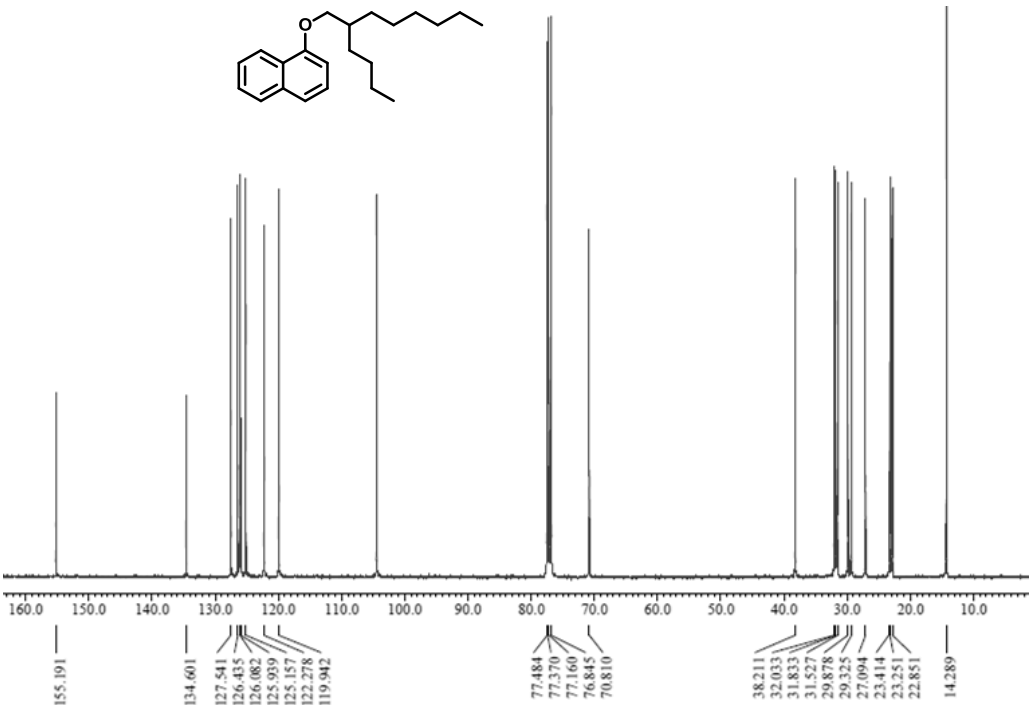

Fig. S2. ^{13}C NMR spectrum of **1**.

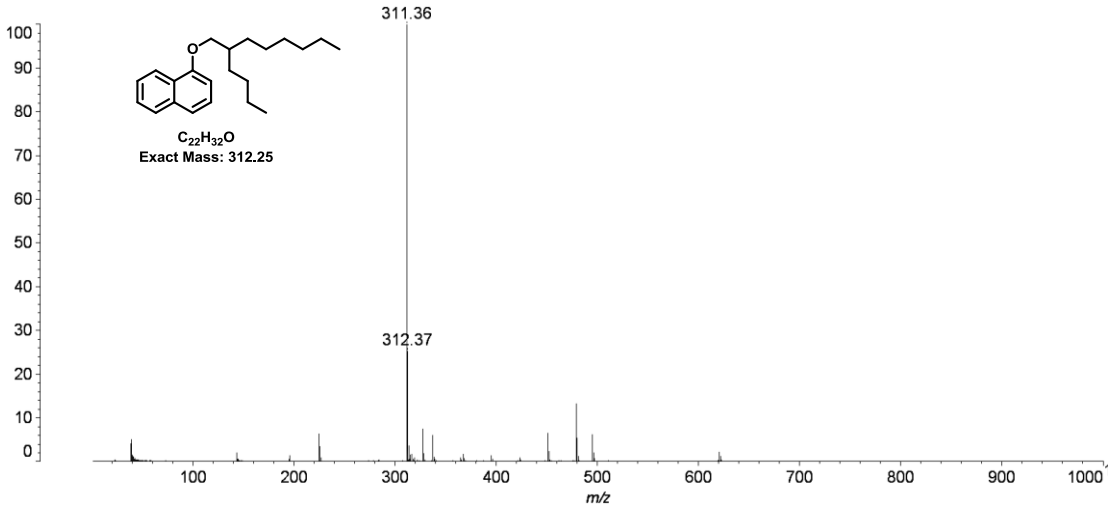

Fig. S3. MALDI-ToF mass spectrum of **1**.

2: Colourless oil; ^{1}H NMR (400 MHz, $CDCl_3$): δ = 7.78-7.68 (m, 3H); 7.43-7.40 (m, 1H); 7.33-7.30 (m, 1H); 7.16-7.11 (m, 2H); 3.95 (d, 2H, J = 5.2 Hz); 1.86-1.82 (m, 1H), 1.47-1.27 (m, 16H), 0.98-0.83 (m, 6H).

^{13}C NMR (100 MHz, $CDCl_3$): δ = 157.5, 134.8, 129.4, 128.9, 127.7, 126.8, 126.4, 123.5, 119.3, 106.5, 71.0, 38.1, 32.0, 31.6, 31.3, 29.9, 29.2, 27.0, 23.3, 22.9, 14.3

MALDI-ToF MS (matrix: dithranol) calculated for $C_{22}H_{32}O$: 312.3, found: 312.4 $[M]^+$.

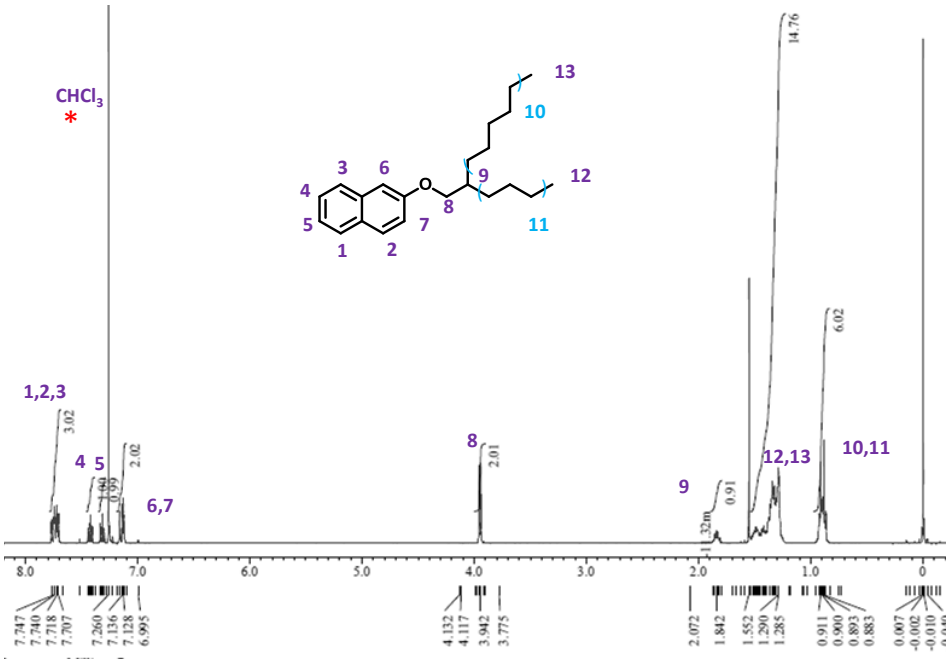

Fig. S4. ^{1}H NMR spectrum of **2**.

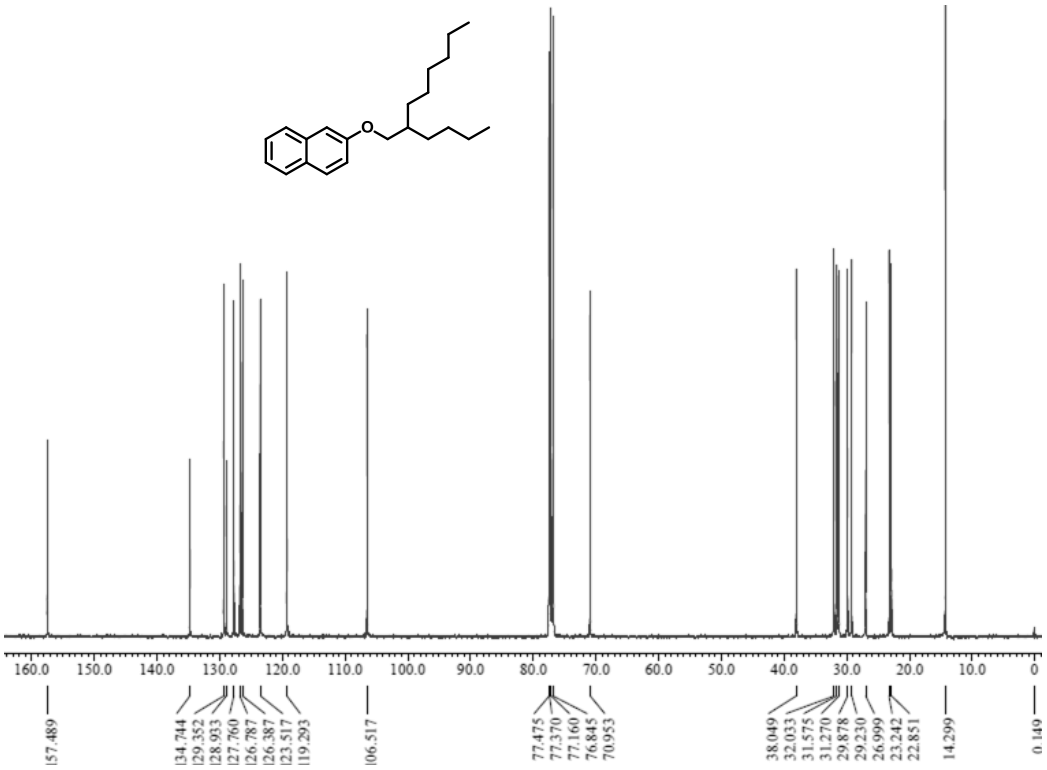

Fig. S5. ^{13}C NMR spectrum of **2**.

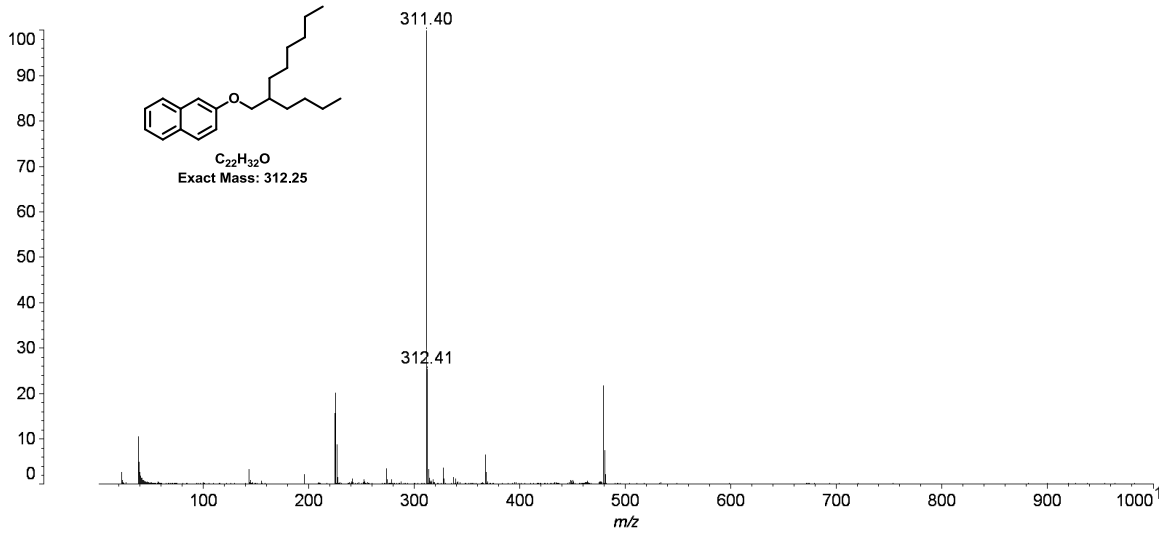

Fig. S6. MALDI-ToF mass spectrum of **2**.

3: Colourless oil; ^{1}H NMR (400 MHz, $CDCl_3$): δ = 8.28 (d, 1H, J = 7.2 Hz); 7.79 (d, 1H, J = 9.2 Hz); 7.50-7.33 (m, 4H); 6.80 (d, 1H, J = 7.6 Hz); 4.02 (d, 2H, J = 5.6 Hz); 1.94-1.90 (m, 1H), 1.53-1.24 (m, 24H), 0.88-0.87 (m, 6H)

^{13}C NMR (100 MHz, $CDCl_3$): δ = 155.2, 134.6, 127.6, 126.4, 126.1, 126.0, 125.2, 122.3, 119.9, 104.5, 70.8, 38.2, 32.1, 32.0, 31.8, 31.6, 30.2, 29.9, 29.5, 27.1, 22.7, 14.3

MALDI-ToF MS (matrix: dithranol) calculated for $C_{26}H_{40}O$: 368.3, found: 368.4 $[M]^+$.

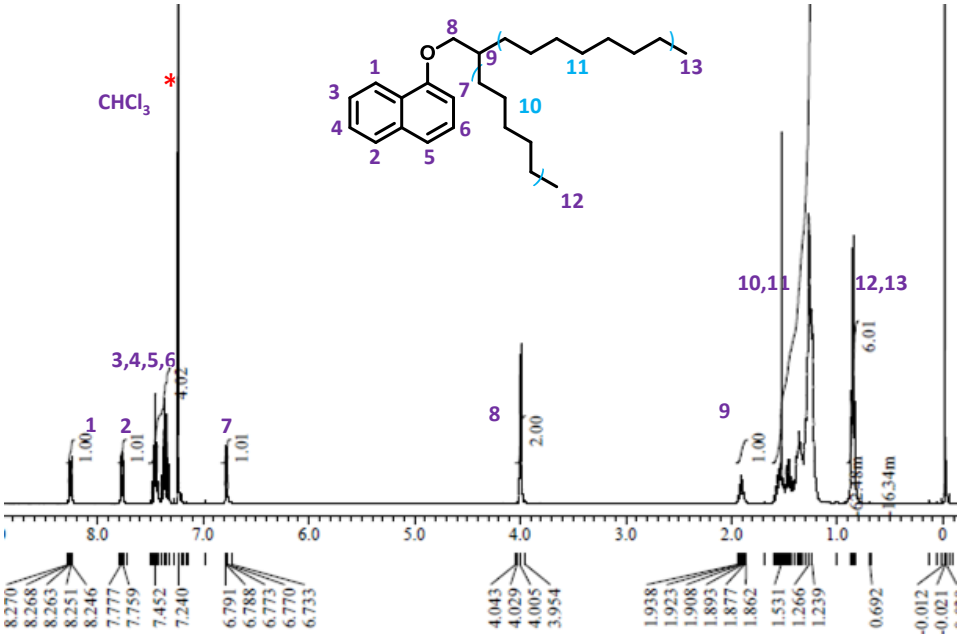

Fig. S7. ^{1}H NMR spectrum of **3**.

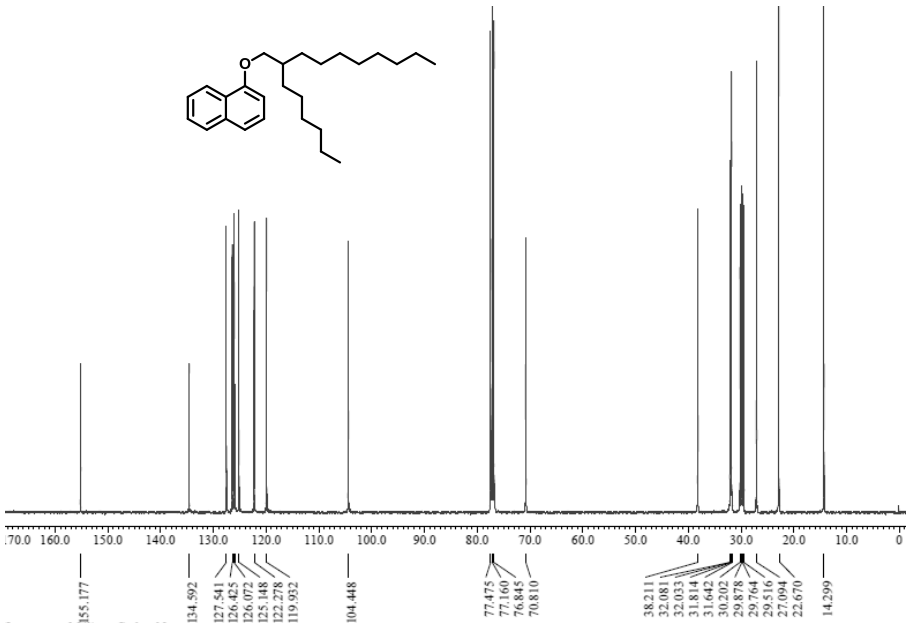

Fig. S8. ^{13}C NMR spectrum of **3.**

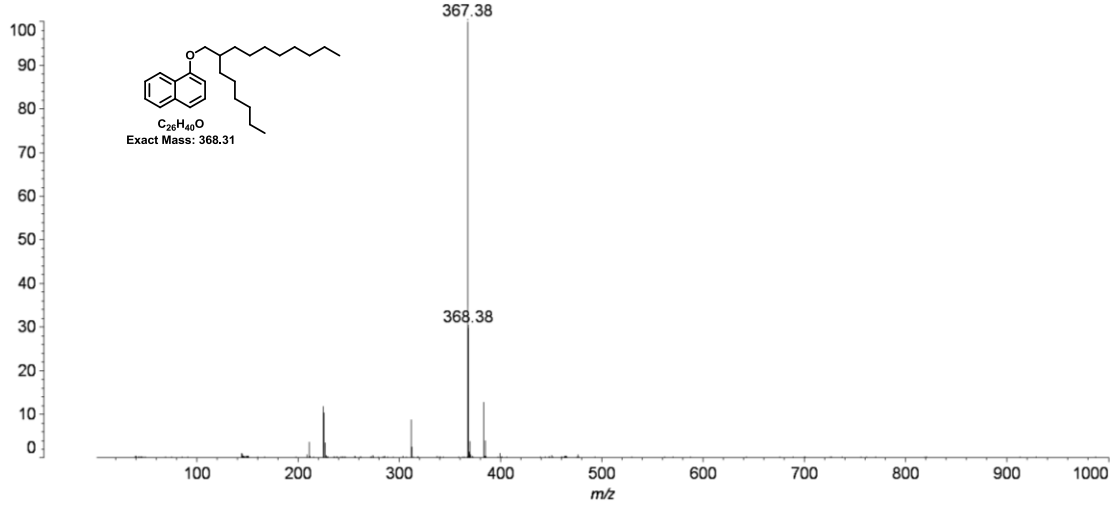

Fig. S9. MALDI-ToF mass spectrum of **3**.

4: Colourless oil; ^{1}H NMR (400 MHz, $CDCl_3$): δ = 7.76-7.70 (m, 3H); 7.44-7.40 (m, 1H); 7.34-7.31 (m, 1H); 7.16-7.13 (m, 2H); 3.96 (d, 2H, J = 5.2 Hz); 1.86-1.80 (m, 1H), 1.48-1.27 (m, 24H), 0.90-0.86 (m, 6H).

^{13}C NMR (100 MHz, $CDCl_3$): δ = 157.5, 134.8, 129.4, 128.9, 127.7, 126.8, 126.4, 123.5, 119.3, 106.5, 71.0, 38.1, 32.0, 31.6, 31.3, 29.9, 29.5, 27.0, 26.9, 22.9, 14.3

MALDI-ToF MS (matrix: *trans* cinnamic acid) calculated for $C_{26}H_{40}O$: 368.3, found: 369.2 $[M+1]^+$.

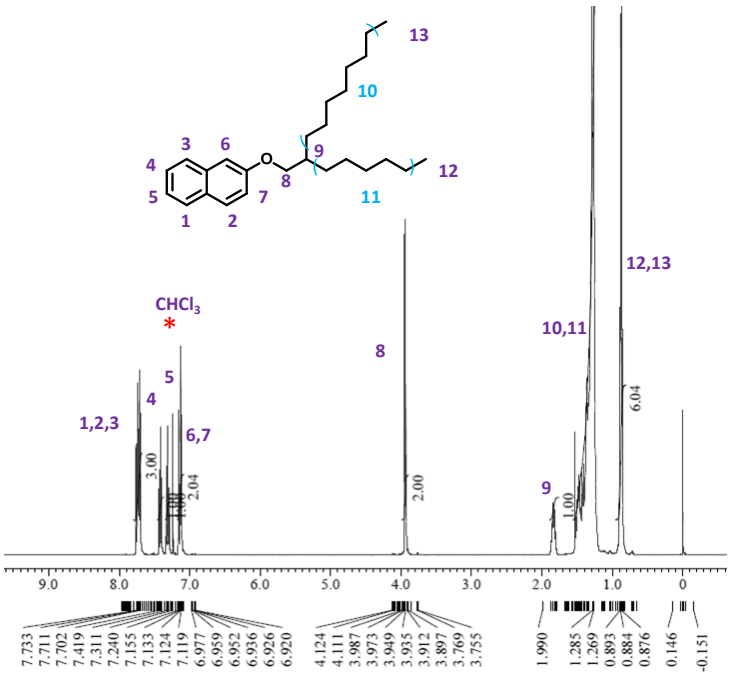

Fig. S10. ^{1}H NMR spectrum of **4**.

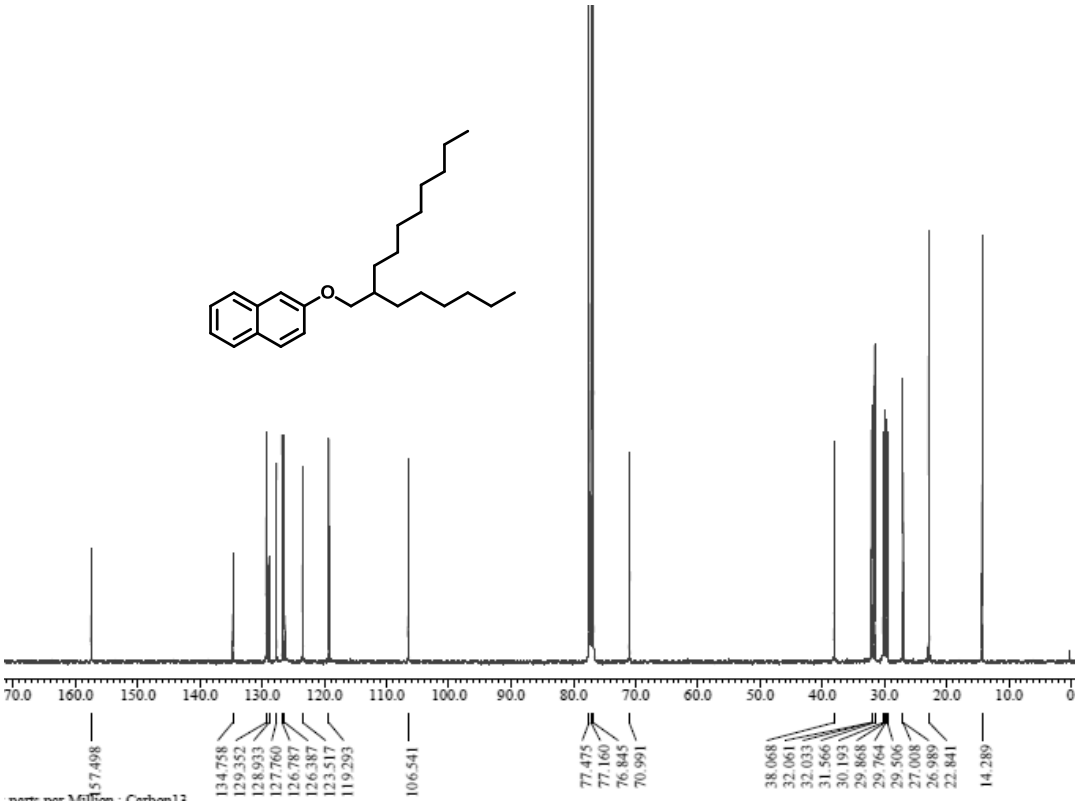

Fig. S11. ^{13}C NMR spectrum of **4.**

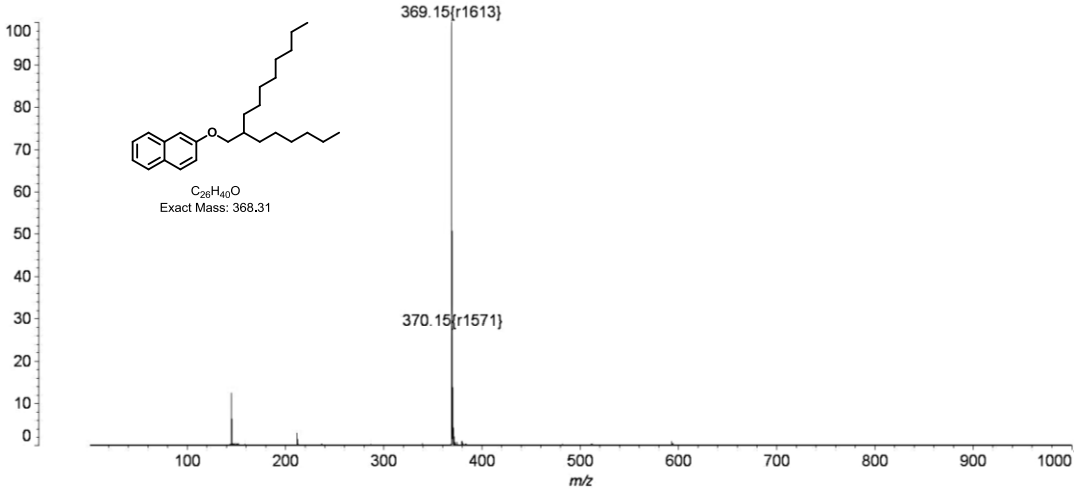

Fig. S12. MALDI-ToF mass spectrum of **4**.

5: Colourless oil; ^{1}H NMR (400 MHz, $CDCl_3$): δ = 8.27 (d, 1H, *J* = 8.2 Hz); 7.78 (d, 1H, *J* = 7.6 Hz); 7.49-7.33 (m, 4H); 6.79 (d, 1H, *J* = 7.2 Hz); 4.00 (d, 2H, *J* = 5.6 Hz); 1.96-1.88 (m, 1H), 1.62-1.25 (m, 32 H), 0.91-0.83 (m, 6H)

^{13}C NMR (100 MHz, $CDCl_3$): δ = 155.2, 134.7, 127.6, 126.4, 126.1, 126.0, 125.2, 122.3, 120.0, 104.5, 70.9, 38.3, 32.1, 32.0, 31.9, 30.2, 29.9, 29.8, 29.7, 29.5, 27.1, 22.9, 14.3

MALDI-ToF MS (matrix: *trans* cinnamic acid) calculated for $C_{30}H_{48}O$: 424.4, found: 424.4 $[M]^+$.

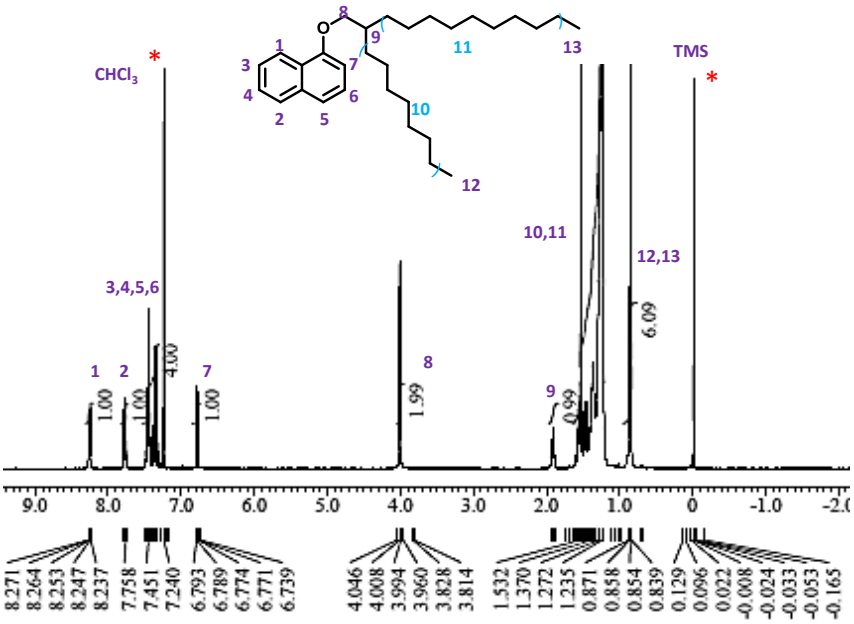

Fig. S13. ^{1}H NMR spectrum of **5**.

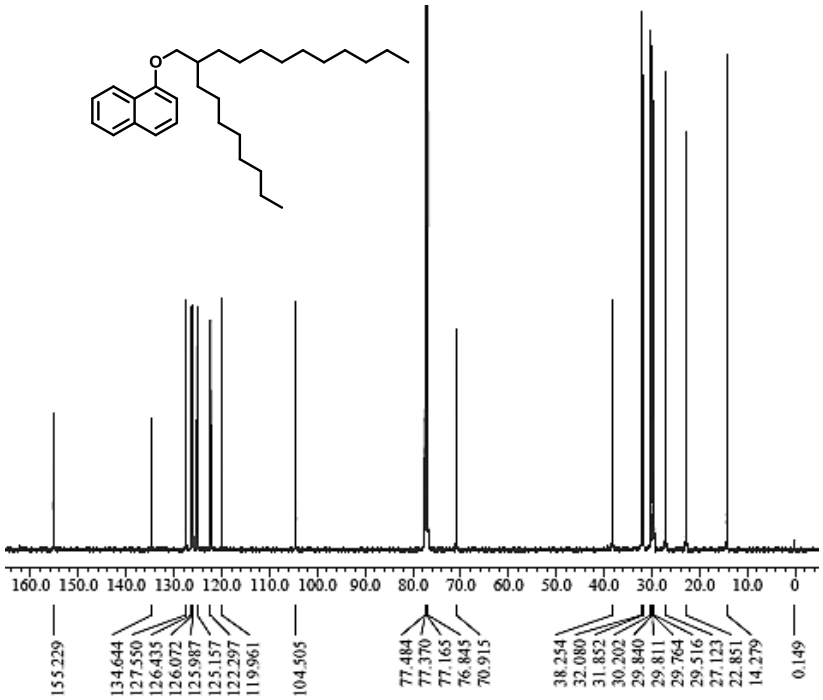

Fig. S14. ^{13}C NMR spectrum of **5**

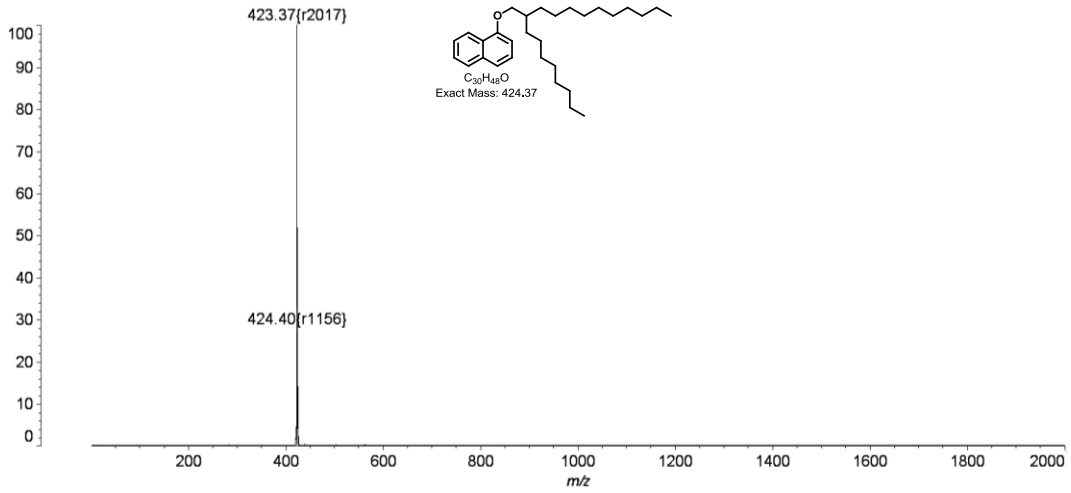

Fig. S15. MALDI-ToF mass spectrum of **5**.

6: Colourless oil; ^{1}H NMR (400 MHz, $CDCl_3$): δ = 7.76-7.70 (m, 3H); 7.43-7.40 (m, 1H); 7.33-7.31 (m, 1H); 7.16-7.13 (m, 2H); 3.95 (d, 2H, J = 5.6 Hz); 1.86-1.82 (m, 1H), 1.48-1.26 (m, 32H), 0.91-0.86 (m, 6H).

^{13}C NMR (100 MHz, $CDCl_3$): δ = 157.5, 134.8, 129.4, 128.9, 127.8, 126.8, 126.4, 123.5, 119.3, 106.6, 71.0, 38.1, 32.1, 31.6, 30.2, 29.9, 29.8, 29.5, 27.0, 26.9, 22.9, 14.3

MALDI-ToF MS (matrix: *trans* cinnamic acid) calculated for $C_{30}H_{48}O$: 424.4, found: 424.0 $[M]^+$.

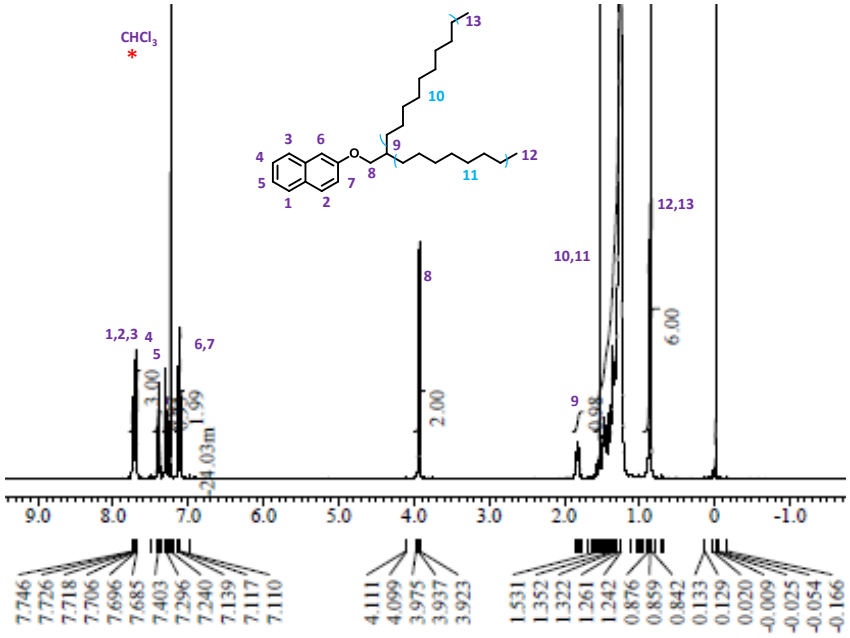

Fig. S16. ^{1}H NMR spectrum of **6**.

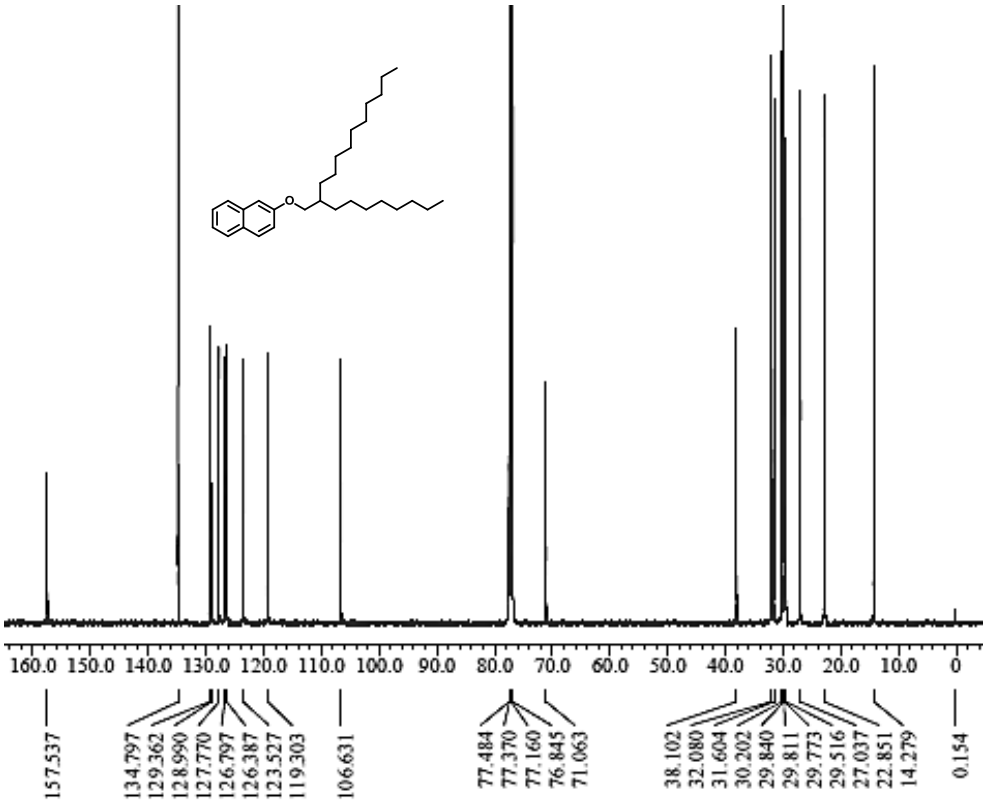

Fig. S17. ^{13}C NMR spectrum of **6**.

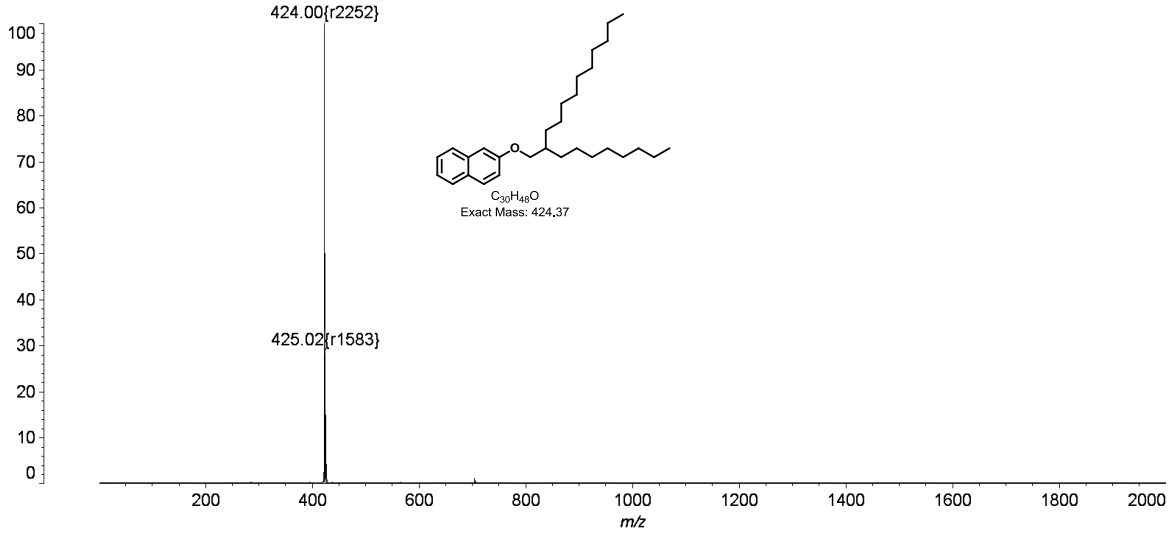

Fig. S18. MALDI-ToF mass spectrum of **6**.

1.3 Techniques

^{1}H and ^{13}C NMR spectra were recorded on a JEOL ECS-400 spectrometer at 400 and 100 MHz, respectively, with tetramethylsilane as the internal standard. All samples were dried up from their dichloromethane solution prior to NMR measurements, to check the presence of any residual solvent. Matrix-assisted laser desorption ionization time-of-flight mass spectra (MALDI-ToF MS) were obtained by a Shimadzu AXIMA-CFR Plus station. Thermogravimetric analysis (TGA) was performed with a Hitachi High-Tech Science TG/DTA 6200 under N_2 flow at a heating rate of 10 °C min^{-1}.

Differential scanning calorimetry (DSC) was measured using Hitachi High-Tech Science DSC7000X with liquid nitrogen cooling accessory under nitrogen gas flow at different scan rates, where noted. Optical microscopy images were obtained under with or without polarized light conditions using an Olympus BX51 optical microscopy, with thin solvent-free liquid layer sandwiched between two glass plates for the measurement. Small and wide angle X-ray scattering (SWAXS) measurements were performed using Anton Paar SAXSess mc^2 instrument.

Rheology experiments were carried out using an Anton Paar Physica MCR301 rheometer, using the parallel plate geometry (50 mm diameter) and a measuring sample thickness of 0.25 mm. For all samples, strain amplitude scans were firstly performed to determine the linear-viscoelastic region. For all samples the strain amplitude of 0.25 was within this linear-viscoelastic region.

For all optical absorption and fluorescence spectroscopy measurements, thin solvent-free liquid samples were sandwiched by two quartz plates. UV-Vis absorption and fluorescence spectra in both solution and solvent-free liquid state were recorded on a JASCO V-670 spectrophotometer and a JASCO FP-8300 spectrophotometer, respectively. Absolute quantum yields were determined on a Hamamatsu Photonics absolute PL quantum yield spectrometer C11347.

Nanosecond time-resolved fluorescence lifetime measurements were carried out by using time-correlated single photon counting (TCSPC) lifetime spectroscopy system HORIBA FluoroCube 3000U-UltraFast-SP spectrophotometer equipped with a nanosecond pulse laser (PB-375L, 375 nm) or nanosecond pulse LED (PB-280, 279 nm) and a nanosecond photon detection module (TBX). Decay analysis and the fitting routine to determine the lifetime(s) were performed using the DAS6 software provided by IBM. The quality of the fit has been judged by the fitting parameters such as chi-squared value $\chi 2$ (< 1.20) as well as the visual inspection of the residuals.

Picosecond time-resolved fluorescence spectra were recorded by using a lab-built spectrometer equipped with a femtosecond Ti:sapphire laser system (Coherent Micra-5/Legend-Elite USP/OPerA Solo, 310 nm), a spectrograph (Acton SP-2358), and a streak camera (Hamamatsu Photonics C10627). Details of the spectrometer have been described elsewhere.[3,4] The pump wavelength was set at 310 nm for all the compounds in the solvent-free liquid state. An α-BBO Glan-Taylor prism analyzer was set

at 54.7° with respect to the polarization of the pump pulse for avoiding spectral changes due to rotational relaxation. Samples were held between two quartz plates and translated every 60 seconds to another spot for avoiding accumulation of photodamage.

All quantum chemical calculations for all compounds were carried out using the Gaussian 09, Revision E.01 suite of programs[5] with default thresholds and algorism. The geometry optimizations of **1**, **2**, and naphthalene in the ground state were performed at the B3LYP/6-311G(d,p) level of theory. The stationary point in the lowest singlet state was optimized without any assumption and characterized by frequency analysis at the same level of theory (the number of imaginary frequencies was 0). The Cartesian coordinates of **1**, **2** and naphthalene are given in Table S2–S4. The time-dependent density functional theory (TD-DFT) calculations at the optimized geometries were conducted at the same level of theory. The natural population analysis calculations[6] at the optimized geometries were conducted at the MP2/6-31G(d) level of theory.

2. Supplementary Tables

Table S1. Photophysical and optical parameters (λ: wavelength; ε: molar absorption coefficient for **1**–**6** in solution and solvent-free liquid state.

Compound	Absorption Features λ_{max}, nm (ε, 10^4 dm^3 mol^{-1} cm^{-1})		Fluorescence λ_{max}, nm	
	Solution[a] (0.1 mM)	Solvent-free liquid[b]	Solution[a] (0.1 mM)	Solvent-free liquid[b]
1	284 (0.56) 294 (0.63) 306 (0.41) 312 (0.32) (sh[c]) 320 (0.21)	287 296 308 313 (sh[c]) 322	322 336 352 371 (sh[c])	327 (sh[c]) 341 356 392
2	253 (0.33) 261 (0.43) 271 (0.45) 282 (0.29) 301 (0.08) (sh[c]) 308 (0.10) (sh[c]) 314 (0.16) 322 (0.14) 329 (0.24) 336 (0.03) (sh[c])	264 274 284 303 (sh[c]) 310 (sh[c]) 316 325 331 (sh[c])	330 (sh[c]) 337 345 351 363 (sh[c])	349 356 379 (sh[c]) 410 (sh[c])
3	285 (0.57) 294 (0.65) 306 (0.42) 311 (0.35) (sh[c]) 321 (0.21)	286 296 308 313 (sh[c]) 322	322 336 352 371 (sh[c])	325 (sh[c]) 339 355 397
4	252 (0.32) 261 (0.41) 271 (0.43) 282 (0.27) 301 (0.07) (sh[c]) 308 (0.09) (sh[c]) 314 (0.16) 322 (0.13) 329 (0.23) 336 (0.03) (sh[c])	264 274 284 303 (sh[c]) 308 (sh[c]) 316 323 331 (sh[c])	330 (sh[c]) 337 345 351 363 (sh[c])	349 355 377 (sh[c]) 409 (sh[c])
5	284 (0.56) 293 (0.64) 306 (0.41) 310 (0.35) (sh[c]) 321 (0.21)	287 296 308 313 (sh[c]) 322	323 337 353 371 (sh[c])	327 (sh[c]) 339 357 378 398 (sh[c])
6	252 (0.37) 261 (0.48) 270 (0.50) 281 (0.32) 300 (0.09) (sh[c]) 307 (0.11) (sh[c]) 313 (0.18) 321 (0.15) 328 (0.24) 335 (0.04) (sh[c])	264 273 284 303 (sh[c]) 308 (sh[c]) 316 322 330 (sh[c])	330 (sh[c]) 338 345 352 363 (sh[c])	348 355 377 (sh[c]) 424 (sh[c])

[a] Prepared in *n*-hexane for all compounds.
[b] Prepared by sandwiching the liquid between two quartz plates.
[c] Shoulder peak.

Table S2. Cartesian coordinates [Å] of the optimized structure for **1**.

atom	X	Y	Z	atom	X	Y	Z
O	-0.974257	-0.635962	-0.615088	H	-0.280159	4.855565	-1.630713
C	-0.020474	-1.182899	-1.531893	H	1.134873	5.481611	-0.778844
H	0.060527	-2.262806	-1.354321	C	5.791442	-0.667211	-0.011627
H	-0.373041	-1.031076	-2.560025	H	5.919632	0.388575	-0.280815
C	1.348795	-0.525766	-1.336029	H	6.464368	-1.230308	-0.67023
H	2.012499	-1.144563	-1.955639	H	-2.046963	-2.556055	-2.204854
C	1.826097	-0.682083	0.123522	C	-2.697678	-2.121583	-1.459166
H	1.714323	-1.739443	0.398596	C	-2.240201	-1.139807	-0.604928
H	1.151413	-0.136076	0.785855	C	-4.902337	-2.049041	-0.447103
C	1.442878	0.891951	-1.956037	C	-3.114354	-0.570322	0.37755
H	1.230702	0.768098	-3.025028	C	-4.036475	-2.571739	-1.370835
H	2.486781	1.223561	-1.908954	C	-4.462771	-1.037062	0.44842
C	3.27596	-0.259053	0.412602	C	-2.681922	0.434474	1.278089
H	3.434039	-0.345938	1.492897	H	-4.370586	-3.34431	-2.054461
H	3.413781	0.802455	0.177881	H	-6.349728	-0.822015	1.474982
C	0.53624	2.026241	-1.432315	H	-5.927042	-2.398224	-0.38659
H	-0.481891	1.653209	-1.292837	C	-3.546186	0.961754	2.209295
H	0.480081	2.778376	-2.22668	H	-1.657975	0.778205	1.221326
C	4.342607	-1.081485	-0.323626	H	-3.202383	1.729713	2.893041
H	4.200519	-2.144785	-0.094479	C	-4.881045	0.506745	2.281081
H	4.195003	-0.988606	-1.405288	H	-5.554511	0.929367	3.018431
C	1.003021	2.721099	-0.144493	C	-5.32518	-0.468825	1.421324
H	1.050813	1.995962	0.672701	C	6.255154	-0.864357	1.441773
H	2.027902	3.090981	-0.283737	H	5.636673	-0.262867	2.116872
C	0.106225	3.889718	0.298801	H	7.270141	-0.461506	1.532408
H	0.427911	4.215671	1.294447	C	6.255894	-2.322675	1.912909
H	-0.922716	3.528375	0.415825	H	6.658014	-2.40768	2.926169
C	0.117667	5.099735	-0.642431	H	6.871844	-2.947859	1.258199
H	-0.49024	5.91467	-0.239787	H	5.249313	-2.749434	1.925053

Table S3. Cartesian coordinates [Å] of the optimized structure for **2**.

atom	X	Y	Z	atom	X	Y	Z
H	-1.878136	1.253528	1.837409	C	3.619541	-0.599747	0.377558
C	-2.552735	0.63757	1.255141	H	3.89306	-0.813846	1.416261
H	-4.285284	1.106026	2.39757	H	3.951423	0.428038	0.190988
C	-3.883308	0.548888	1.557713	C	1.212225	2.336046	-1.088778
C	-2.832053	-0.887224	-0.611024	H	0.127491	2.225124	-1.003667
C	-4.761054	-0.264793	0.79028	H	1.381678	3.131555	-1.823133
C	-2.013923	-0.088065	0.157847	C	4.379649	-1.553149	-0.554714
C	-4.218187	-0.993541	-0.312568	H	4.034455	-2.579808	-0.380935
C	-6.143355	-0.376362	1.079867	H	4.125187	-1.326864	-1.596039
H	-4.684527	-2.362209	-1.920539	C	1.77357	2.794046	0.264574
H	-2.443496	-1.445381	-1.452421	H	1.555372	2.039917	1.024782
C	-6.962966	-1.173049	0.315565	H	2.86795	2.863863	0.202424
H	-6.547028	0.180441	1.919476	C	1.213922	4.142368	0.749712
H	-8.019266	-1.250759	0.546439	H	1.534328	4.298919	1.785925
C	-6.428363	-1.89411	-0.775569	H	0.118697	4.086515	0.777185
H	-7.080272	-2.520532	-1.374386	C	1.642942	5.354108	-0.085643
C	-5.090661	-1.806505	-1.081505	H	1.256374	6.282806	0.343326
O	-0.677009	0.089256	-0.03699	H	1.278083	5.29487	-1.114309
C	-0.03393	-0.627502	-1.095612	H	2.734112	5.436856	-0.125023
H	-0.202567	-1.702255	-0.950281	C	5.911227	-1.485647	-0.421089
H	-0.479109	-0.33928	-2.056814	H	6.235633	-0.457494	-0.624212
C	1.468453	-0.334773	-1.091634	H	6.357738	-2.104102	-1.209642
H	1.870381	-1.058261	-1.814128	C	6.493653	-1.927776	0.932281
C	2.087742	-0.687636	0.278655	H	6.106099	-1.288972	1.733424
H	1.785848	-1.715505	0.521465	H	7.575089	-1.752436	0.910806
H	1.64119	-0.060915	1.052292	C	6.236165	-3.397715	1.281156
C	1.822993	1.052486	-1.687223	H	6.729272	-3.67111	2.218036
H	1.523238	1.015699	-2.741912	H	6.619456	-4.061087	0.498892
H	2.914163	1.154808	-1.703499	H	5.170151	-3.609702	1.400229

Table S4. Cartesian coordinates [Å] of the optimized structure for naphthalene.

atom	X	Y	Z
H	-3.372235	0.000032	-1.242819
C	-2.429436	0.000009	-0.707401
H	-1.241863	0.000024	-2.48541
C	-1.243502	0.000012	-1.400221
C	-1.243502	-0.000012	1.400221
C	0	0	-0.715722
C	-2.429436	-0.000009	0.707401
C	0	0	0.715722
C	1.243502	-0.000012	-1.400221

atom	X	Y	Z
H	-3.372235	-0.000032	1.242819
H	1.241863	0.000024	2.48541
H	-1.241863	-0.000024	2.48541
C	2.429436	-0.000009	-0.707401
H	1.241863	-0.000024	-2.48541
H	3.372235	-0.000032	-1.242819
C	2.429436	0.000009	0.707401
H	3.372235	0.000032	1.242819
C	1.243502	0.000012	1.400221

3. Supplementary Figures

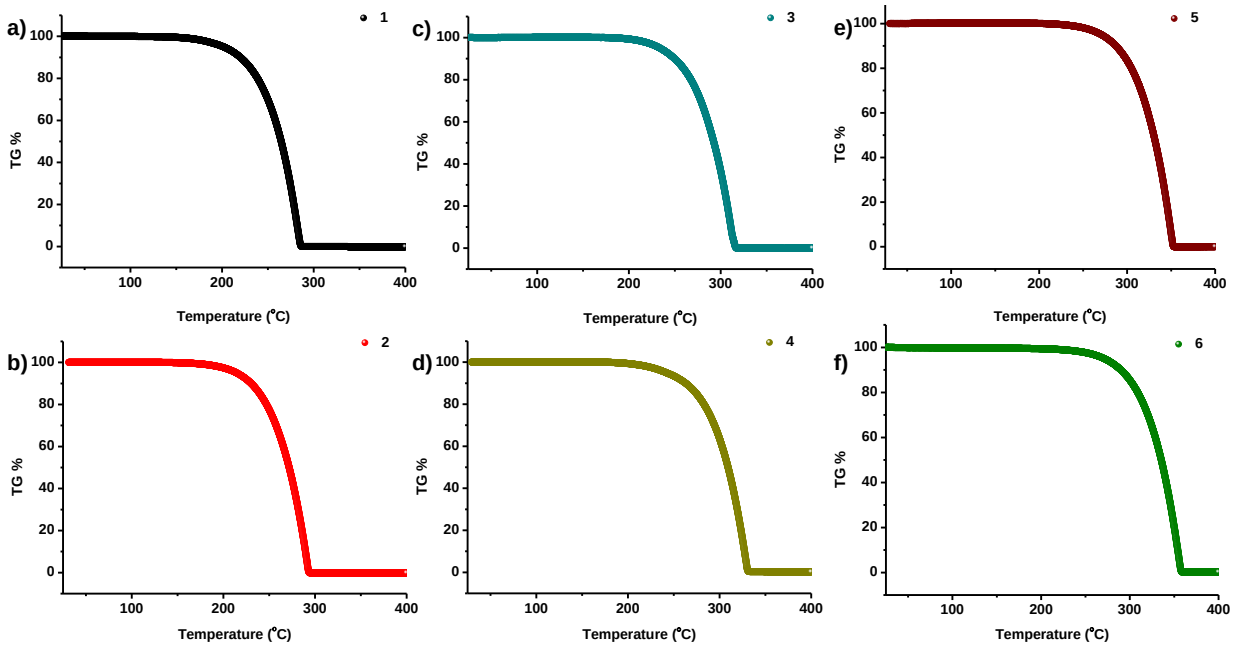

Fig. S19. Thermogravimetric profiles of **1** (a), **2** (b), **3** (c), **4** (d), **5** (e), **6** (f) respectively, indicating absence of residual solvents in the bulk fluid. The heating rate is 10 °C min^{-1}.

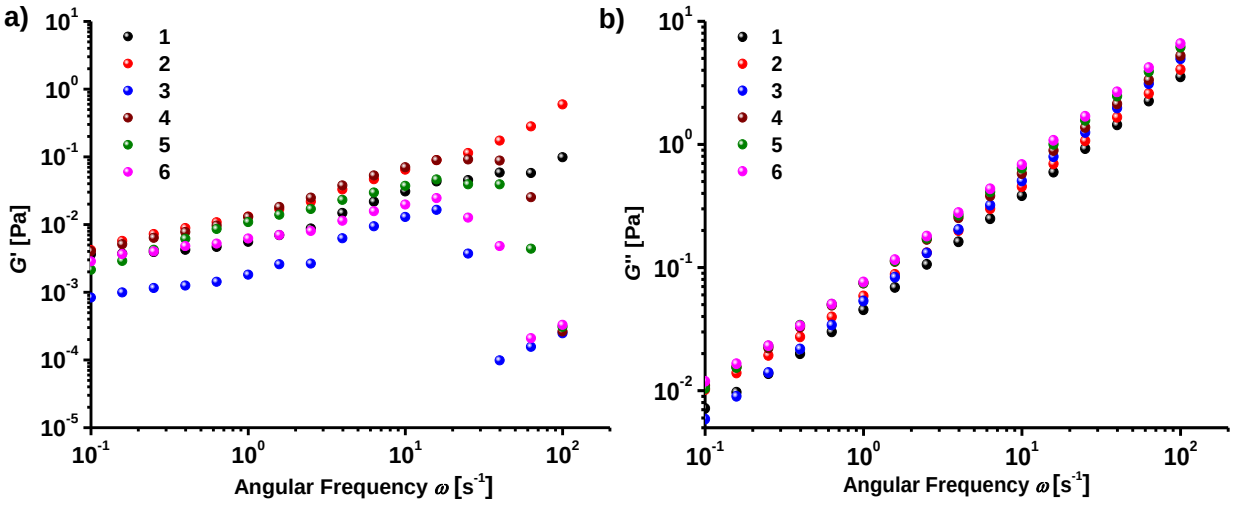

Fig. S20. Rheology analysis of **1**-**6** at solvent-free liquid state. Variation of (a) storage modulus (*G*') and (b) loss modulus (*G*'') with frequency sweep at a constant amplitude strain of 25%. The *G*' values were found to be lower than the *G*'' for all compounds, depicting the liquid nature.

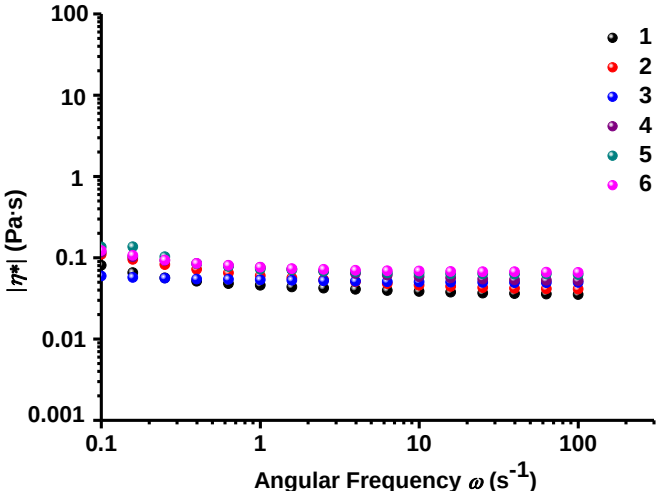

Fig. S21. Complex viscosities (η^*) versus angular frequency (ω) plots for **1**–**6** at solvent-free liquid state (25 °C, ω = 10 rad s^{-1}), demonstrating the Newtonian liquid behaviour.

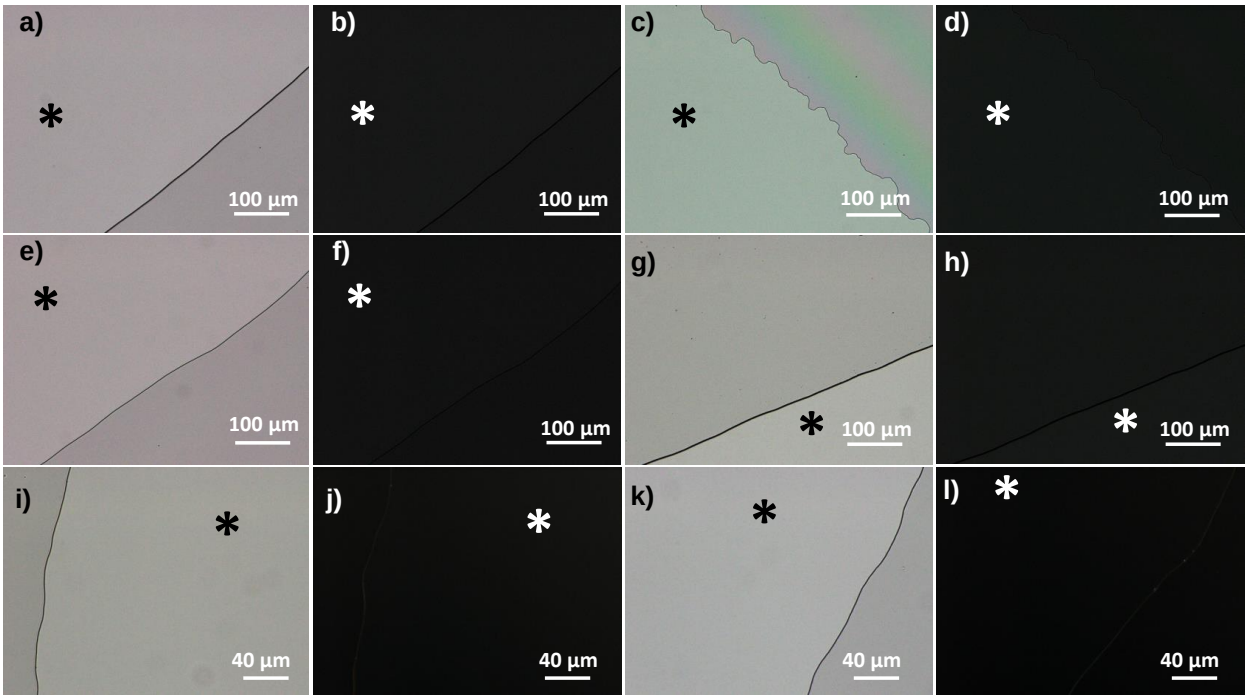

Fig. S22. Optical microscopy (OM) (a, c, e, g, i, k) and polarized optical microscopy (POM) images (b, d, f, h, j, l) of the liquid naphthalenes, of **1** (a, b), **2** (c, d), **3** (e, f), **4** (g, h), **5** (i, j), **6** (k, l). The regions marked with asterisk (*) represent the sample.

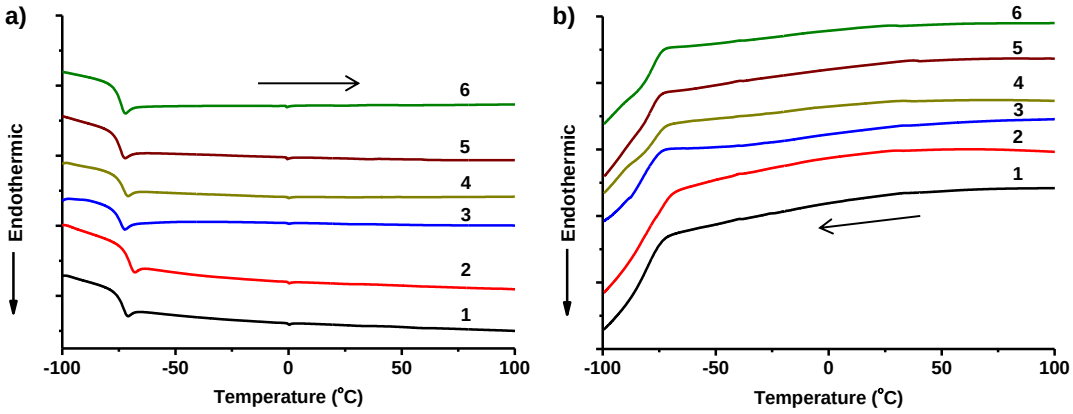

Fig. S23. Differential scanning calorimetry (DSC) curves, (a) heating traces and (b) cooling traces, of **1**–**6**. The heating and cooling rates are 10 °C min^{-1}.

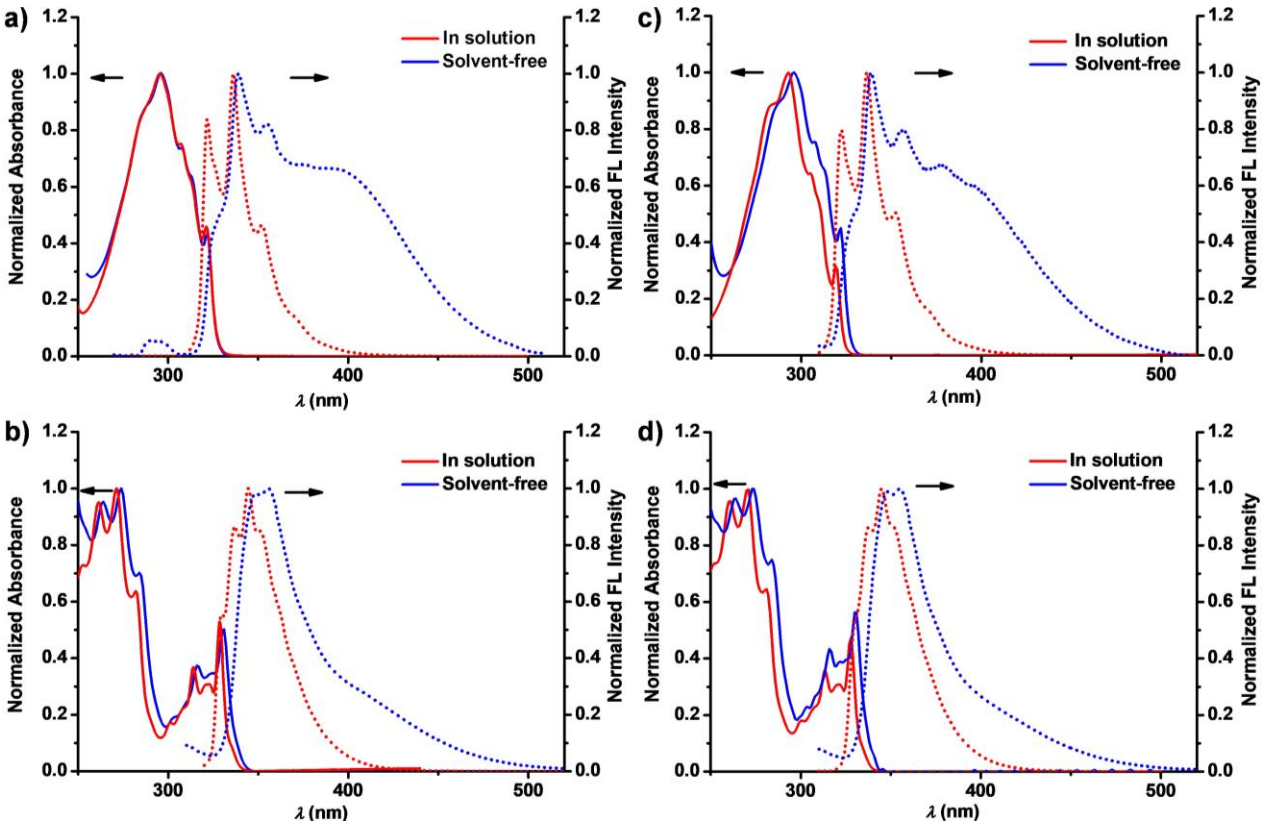

Fig. S24. Normalized UV-visible absorption (solid lines) and fluorescence (dotted lines) of **3** (a), **4** (b), **5** (c), **6** (d) in *n*-hexane ([*c*] = 0.1 mM, red lines) and in solvent-free liquid state (blue lines). Arrows have been provided to guide the eye.

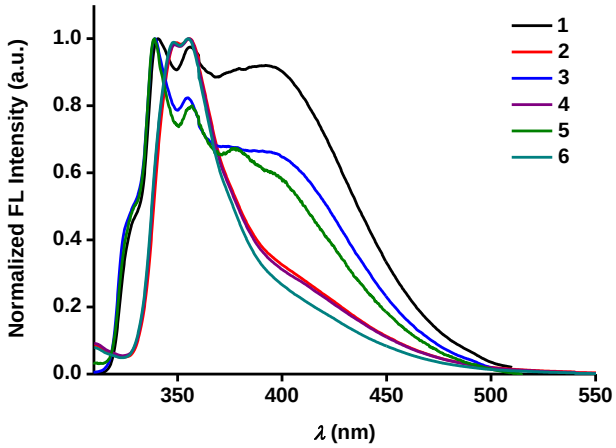

Fig. S25. Overlaid emission profiles of alkylated-naphthalenes (**1**–**6**) in solvent-free liquid state. The excimer formation tendency of the 1-substituted regioisomers (**1**, **3**, **5**) is higher than the 2-substituted regioisomers (**2**, **4**, **6**). It decreases with the increase in the chain length.

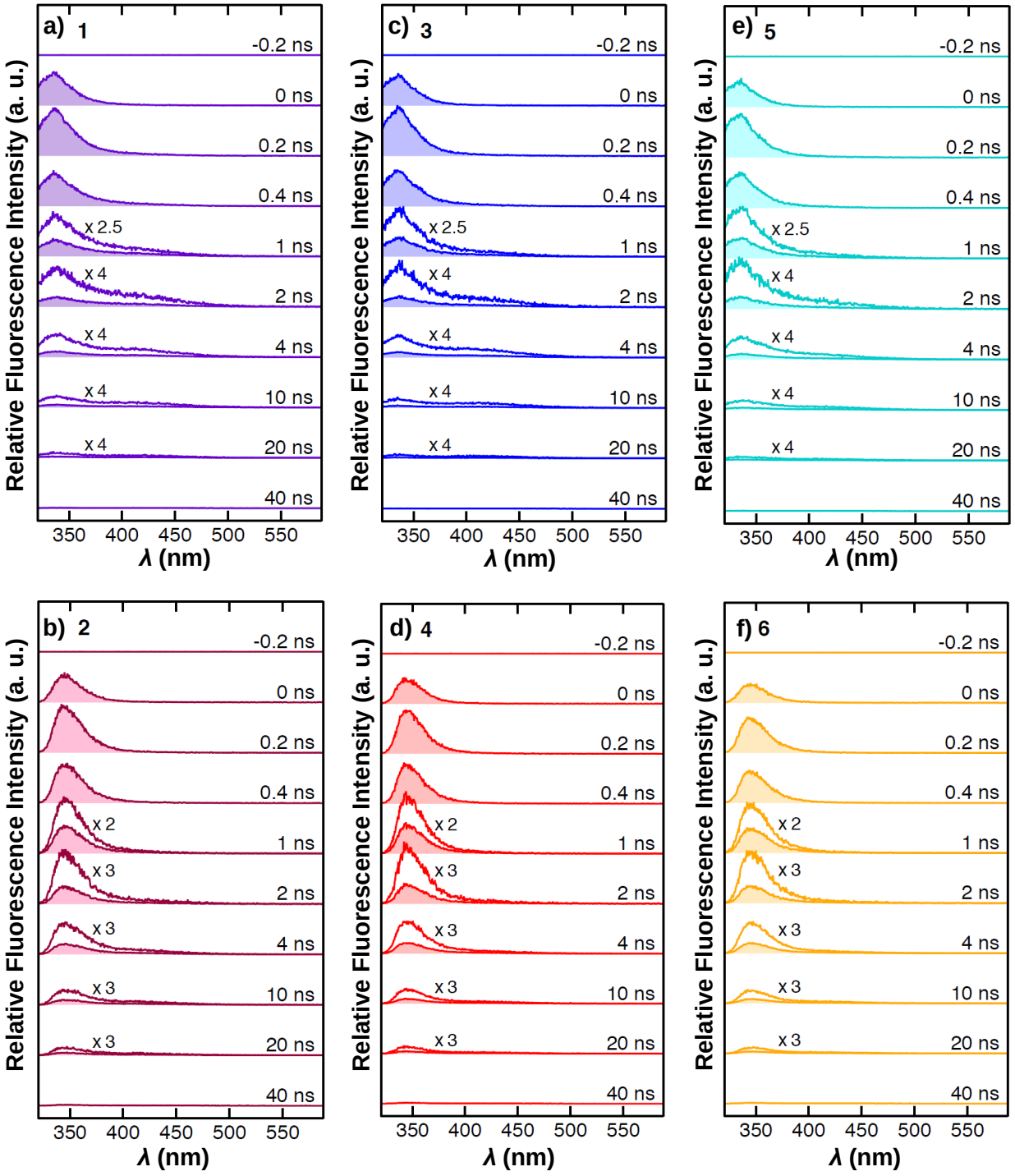

Fig. S26. Picosecond time-resolved fluorescence spectra of **1** (a), **2** (b), **3** (c), **4** (d), **5** (e), **6** (f) respectively in the solvent-free liquid state with photoexcitation at 310 nm.

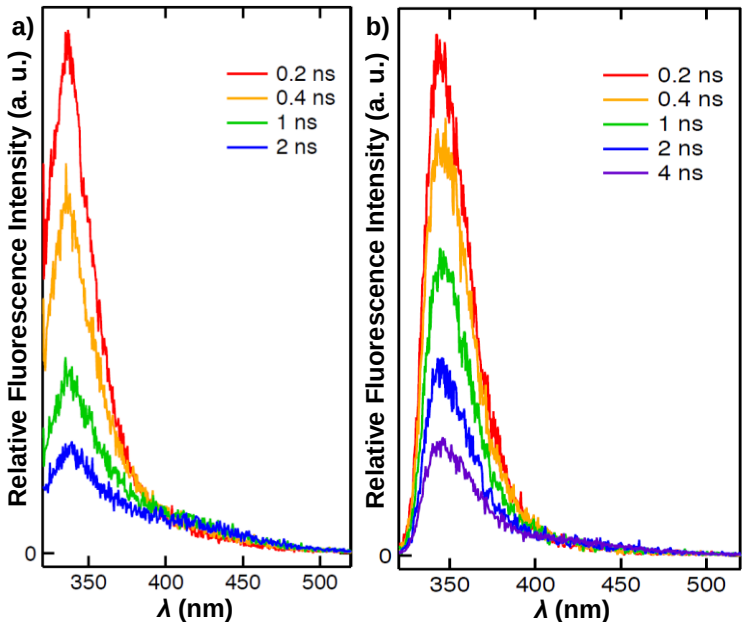

Fig. S27. Superimposed time-resolved fluorescence spectra of **1** (a) and **2** (b) in the solvent-free liquid state. An isoemissive point is observed at around 400 nm for both of the samples.

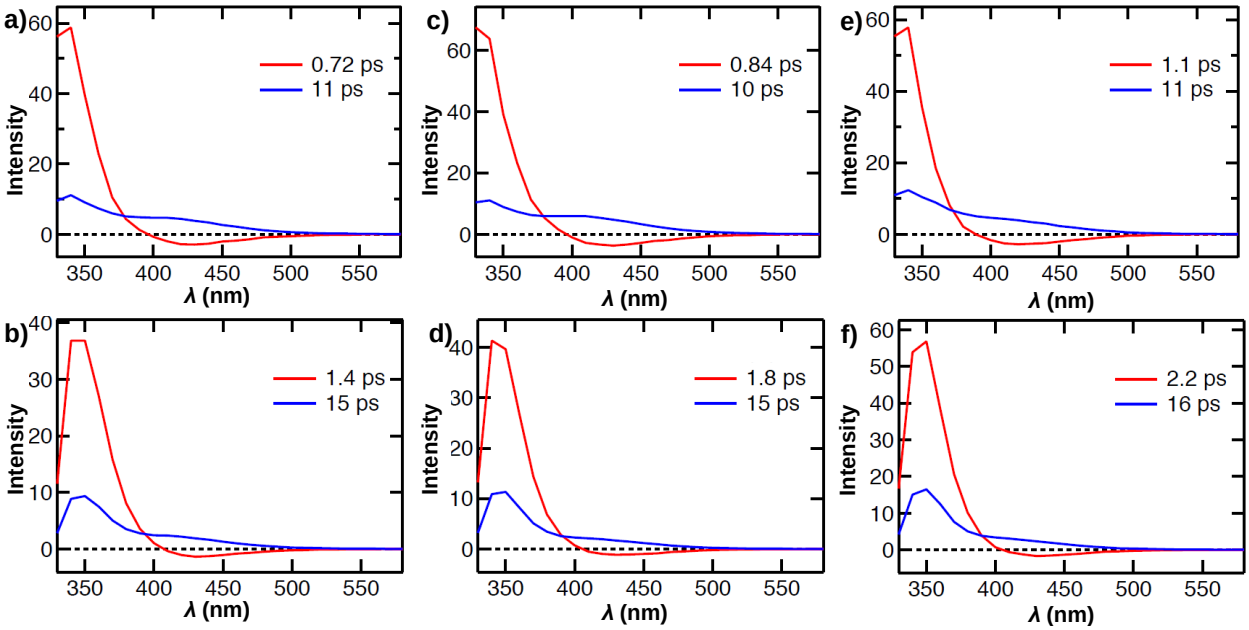

Fig. S28. Fluorescence decay associated spectra of **1** (a), **2** (b), **3** (c), **4** (d), **5** (e), **6** (f) respectively in the solvent-free liquid state with photoexcitation at 310 nm obtained by the global least-squares fitting analysis in 330–580 nm.

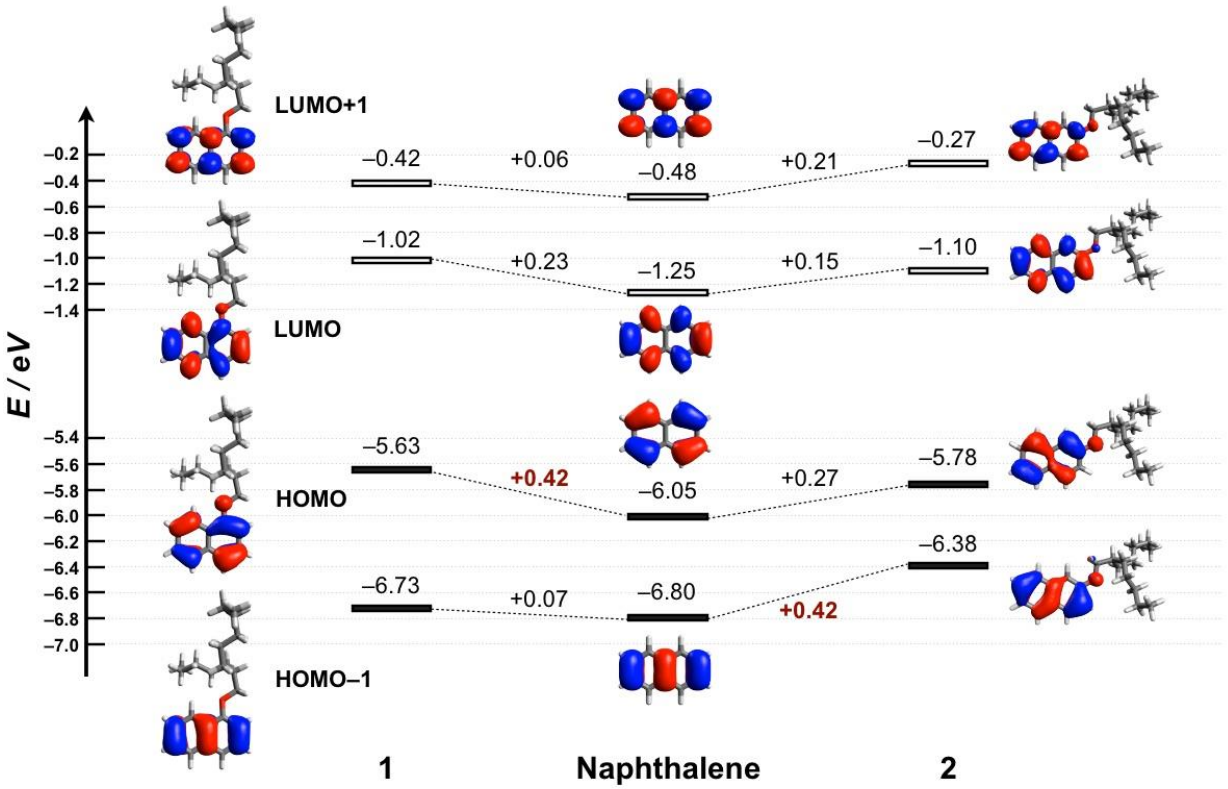

Fig. S29. The electronic effects of alkyloxy group to naphthalene skeleton at 1- and 2-positions, calculated at B3LYP/6-311G(d,p) level. The electronic perturbations of alkyloxy group are highly dependent on the orbital coefficients at 1- and 2-positions of naphthalene. For example, **1** has higher HOMO level than **2**, due to their large orbital coefficient at 1-position of naphthalene in the HOMO level. On the other hand, the LUMO levels, which have similar orbital coefficients at 1- and 2-positions, are comparable in **1** and **2**. The incensed energy levels clearly suggest that these alkyloxy substituents work as electron-donating groups in both cases. In addition, while **1** keeps the similar MOs with pristine naphthalene, **2** possesses asymmetric MOs. These differences presumably reflect to a slight difference in the dipole moment.

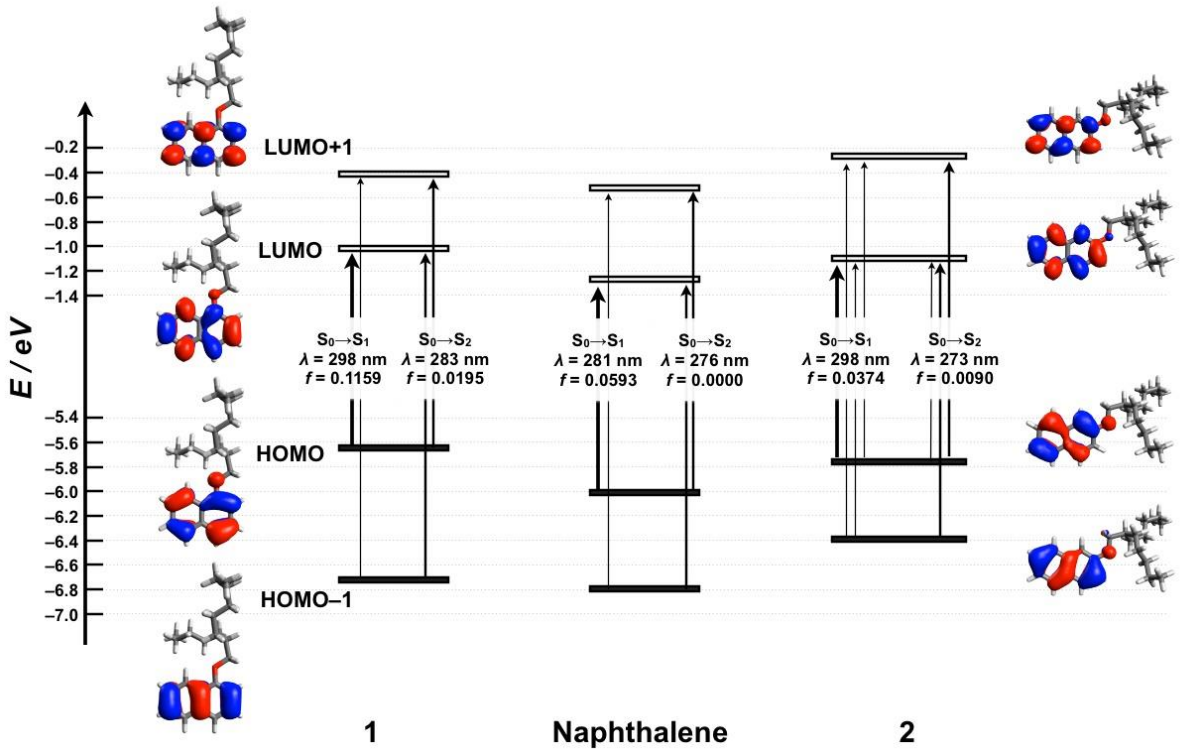

Fig. S30. Estimated electronic transitions of **1** and **2** calculated by TD-DFT calculations at the B3LYP/6-311G(d,p)//B3LYP/6-311G(d,p) level. Alkylation makes both transitions from S_0 to S_1 and from S_0 to S_2 allowed due to the asymmetric molecular structures. Particularly, the electronic transitions of **2** contain distinct contributions from those of **1**. This result clearly supports the distinct absorption spectra of **2** from **1** in *n*-hexane solution.

References

[1] T. Aytun, L. Barreda, A. Ruiz-Carretero, J. A. Lehrman and S. I. Stupp*, Chem. Mater.*, 2015, **27**, 1201−1209.

[2] S. Choi, G. E. Park, D. H. Lee, M. Godumala, M. J. Cho and D. H. Choi, *J. Pol. Sci. A: Poly. Chem.*, 2017, **55**, 1209-1218; M. C. Hwang, J.-W. Jang, T. K. An, C. E. Park, Y.-H. Kim and S.-K. Kwon, *Macromol.*, 2012, **45**, 4520−4528.

[3] F. Lu, T. Takaya, K. Iwata, I. Kawamura, A. Saeki, M. Ishii, K. Nagura and T. Nakanishi, *Sci. Rep.*, 2017, **7**, 3416.

[4] Y. Nojima and K. Iwata, *J. Phys. Chem. B*, 2014, **118**, 8631.

[5] M. J. Frisch, G. W. Trucks, H. B. Schlegel, G. E. Scuseria, M. A. Robb, J. R. Cheeseman, G. Scalmani, V. Barone, B. Mennucci, G. A. Petersson, H. Nakatsuji, M. Caricato, X. Li, H. P. Hratchian, A. F. Izmaylov, J. Bloino, G. Zheng, J. L. Sonnenberg, M. Hada, M. Ehara, K. Toyota, R. Fukuda, J. Hasegawa, M. Ishida, T. Nakajima, Y. Honda, O. Kitao, H. Nakai, T. Vreven, J. A. Montgomery, Jr., J. E. Peralta, F. Ogliaro, M. Bearpark, J. J. Heyd, E. Brothers, K. N. Kudin, V. N. Staroverov, T. Keith, R. Kobayashi, J. Normand, K. Raghavachari, A. Rendell, J. C. Burant, S. S. Iyengar, J. Tomasi, M. Cossi, N. Rega, J. M. Millam, M. Klene, J. E. Knox, J. B. Cross, V. Bakken, C. Adamo, J. Jaramillo, R. Gomperts, R. E. Stratmann, O. Yazyev, A. J. Austin, R. Cammi, C. Pomelli, J. W. Ochterski, R. L. Martin, K. Morokuma, V. G. Zakrzewski, G. A. Voth, P. Salvador, J. J. Dannenberg, S. Dapprich, A. D. Daniels, O. Farkas, J. B. Foresman, J. V. Ortiz, J. Cioslowski, and D. J. Fox, Gaussian 09, Revision E.01, Gaussian, Inc., Wallingford CT, 2013.

[6] E. D. Glendening, A. E. Reed, J. E. Carpenter, and F. Weinhold, NBO Version 3.1.